

Tuning and sensing spin interactions in Co-porphyrin/Au with NH₃ and NO₂ bindingMin Hui Chang,^{1,*} Yun Hee Chang,^{2,*} Na-Young Kim,² Howon Kim,³ Soon-Hyeong Lee,¹ Mahn-Soo Choi,¹ Yong-Hyun Kim,^{2,4,†} and Se-Jong Kahng^{1,‡}¹*Department of Physics, Korea University, 145 Anam-ro, Seongbuk-gu, Seoul 02841, Republic of Korea*²*Graduate School of Nanoscience and Technology, KAIST, Daejeon 34141, Republic of Korea*³*Department of Physics, University of Hamburg, D-20355 Hamburg, Germany*⁴*Department of Physics, KAIST, Daejeon 34141, Republic of Korea*

(Received 2 August 2019; published 6 December 2019)

Controlling spin interactions in magnetic-molecules/metal is essential for spintronic applications. Recent studies showed that using small molecule coordination, one could switch off the spin interactions between magnetic-molecules and metal substrates. However, this control should not be limited to the two-state switching. The strength of spin interaction can be reduced, but not “off” by the proper selection of small molecules. To demonstrate this, we considered two contrasting systems, NH₃ and NO₂ coordinated to Co-porphyrin/Au(111). In our scanning tunneling microscopy and spectroscopy (STM and STS), Kondo resonance was preserved with weakened spin coupling after NH₃ coordination. However, it disappeared after NO₂ coordination, implying “off” spin coupling. These observations are explained with our density functional theory calculation results. This study shows that small molecule coordination to magnetic-molecules/metal is a powerful way to control spin interactions at the single-molecule level.

DOI: [10.1103/PhysRevB.100.245406](https://doi.org/10.1103/PhysRevB.100.245406)**I. INTRODUCTION**

The central metal atom in metalloporphyrins and phthalocyanines often forms a six-coordination structure that plays important roles in biological processes such as oxygen transfer, muscle contraction, and photosynthesis cycles. Among the six coordinated ligands, two out-of-plane ones compete with each other to make a stronger bond with less chemical reactivity than the other, which is known as trans effect [1–5]. The winners of the competitions are mostly determined by their charge donation ability, and the order is known as NO > CH₃ > SO₃²⁻ > NO₂ > Br > Cl > NH₃ > OH > vacuum, where vacuum means no ligand [3–5]. Recently, metallic surfaces are included in the ligand list, and those cases are named surface trans effect [6–26]. An example is Co-porphyrin (CoP)/Ag and NO-CoP/Ag. In the former, Ag surface forms stronger bond to CoP because of no competition than in the latter [6,8].

On ferromagnetic surfaces, the surface trans effect provides a way to switch the magnetic interaction between the surface and the metallomolecule, and is specifically called spin trans effect [27–43]. It can be seen in CoP/Ni and NO-CoP/Ni. The former has the ferromagnetic interaction between CoP and Ni substrate, but the latter has it “off,” as measured with x-ray magnetic circular dichroism (XMCD) [28,32]. Our group reported scanning tunneling microscopy (STM) and spectroscopy (STS) results for CoP/Au and NO-CoP/Au, showing the spin trans effect on the nonmagnetic Au

surface, where spin exchange coupling between unpaired spin in Co and conduction electrons in the Au surface was expected to induce Kondo resonance [34,37,39].

The main focus in previous spin trans effect studies was to manifest theoretically predicted “on” and “off” switching capability for spin interactions or moments by small molecules coordination [28–30,32–34,38,39]. In fact, this controlling is not necessarily limited to the two-state switching. There are much more degrees of freedom; by the choice of proper molecule, the spin interactions can be reduced with lower Kondo temperature, or switched off, as depicted in Fig. 1. X-ray standing wave (XSW) and XMCD experiments showed the coordination of NH₃ to Mn-phthalocyanines induced a modification of spin interactions [35,36]. Reports that manifest such possibility at the single molecule level are not available in the literature.

In this paper, we present STM and STS results of two contrasting systems, NH₃ and NO₂ coordinated to tetrakis-phenylporphyrin-Co (CoTPP)/Au(111). We have selected the two molecules considering the order of ligands’ charge donation ability mentioned above; NH₃ and NO₂ are in-between the two extremes of NO and vacuum. With NH₃ coordination, we observed that a zero-bias peak at CoTPP, a signature of the Kondo effect in STS, was remained but showed a reduced width, namely, the reduced Kondo temperature. With NO₂ coordination, no zero-bias peak was resolved. We have also shown that single NH₃ and NO₂ molecules can be decoordinated from CoTPP using STM manipulations. The observed results are explained by the spatial redistribution of unpaired spins in the *d*_{z²} orbitals of CoTPP by NH₃ and NO₂ coordination from our density functional theory (DFT) calculation results [44].

*These authors contributed equally.

†yong.hyun.kim@kaist.ac.kr

‡sjkahng@korea.ac.kr

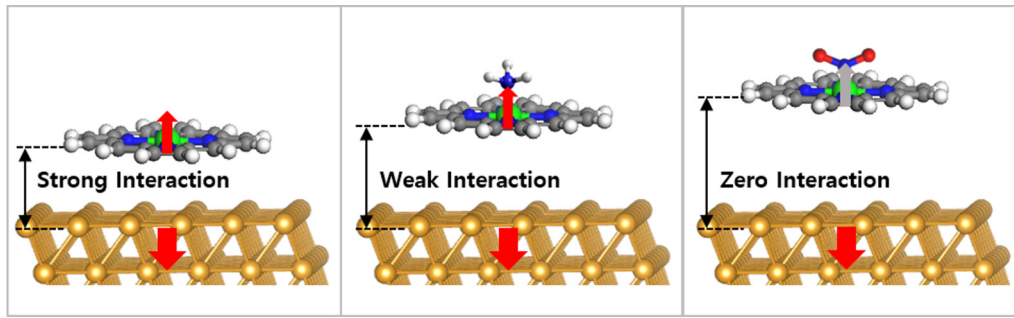


FIG. 1. Controlling spin exchange interactions. Schematic diagrams to depict how spin exchange interactions between metalloporphyrin and Au(111) can be controlled by small molecule coordination. The charge donation ability of small molecules is known to be vacuum $< \text{NH}_3 < \text{NO}_2$. With NH_3 coordination, the exchange interaction will be weakened because of the increased distance between metalloporphyrin and Au(111), resulting in reduced Kondo temperature. With NO_2 coordination, the exchange interaction will be even more weakened, resulting in absent Kondo resonance.

II. RESULTS AND DISCUSSION

CoTPP and H_2TPP (H_2 -tetrakis-phenylporphyrin) were prepared as randomly-mixed molecular islands on Au(111), and then whole sample was exposed to NH_3 gas at 80 K. In separate experiments, similarly prepared sample of CoTPP and H_2TPP was exposed to NO_2 gas. Figures 2(a)–2(d) show

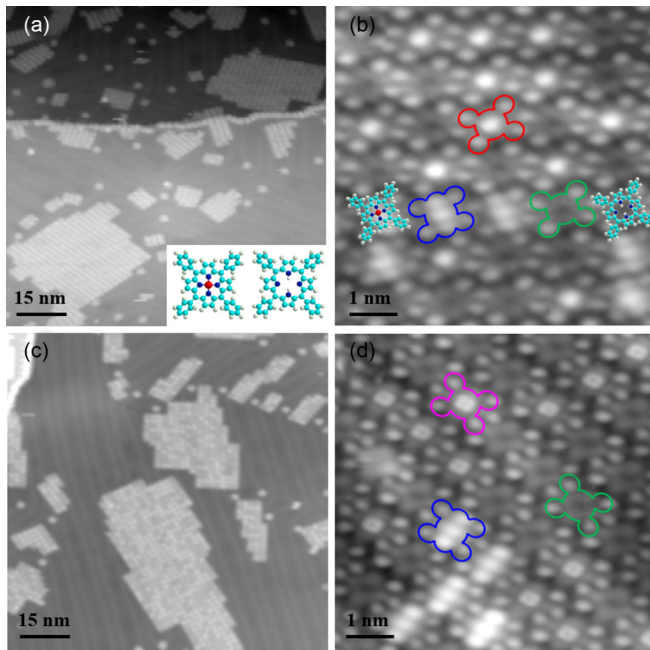


FIG. 2. NH_3 and NO_2 coordination to CoTPP on Au(111). (a), (b) Typical STM images of mixed molecular islands of CoTPP and H_2TPP on the Au(111) surface after exposure to NH_3 gas. (c), (d) STM images of mixed molecular islands of CoTPP and H_2TPP on the Au(111) surface after exposure to NO_2 gas. The four representative molecules of CoTPP, H_2TPP , NH_3 -CoTPP, and NO_2 -CoTPP are denoted by blue, green, red, and pink marks, respectively, in (b) and (d). Inset of (a): Ball and stick models of CoTPP and H_2TPP molecules. The cyan, blue, red, and white circles denote carbon, nitrogen, cobalt, and hydrogen atoms, respectively. The sizes of STM images: (a) and (c) $96 \times 96 \text{ nm}^2$, (b) and (d) $11 \times 11 \text{ nm}^2$. Tunneling current: $I_T = 0.1 \text{ nA}$. Sample voltage: (a), (c), (d) $V_S = -0.3 \text{ V}$, (b) $V_S = -0.2 \text{ V}$.

typical STM images obtained at 80 K after gas exposure. We observed three different molecules in both experiments with NH_3 and NO_2 gas. Because CoTPP shows a three-lobed shape and H_2TPP shows a depressed-center structure at -0.5 eV in the STM images [34,45–47], it was straightforward to identify CoTPP, H_2TPP , and the third molecules. In Figs. 2(b) and 2(d), CoTPP and H_2TPP are marked with green and blue, respectively, and the third molecules are marked with red or pink. We consider the third molecules as gas-adsorbed porphyrin molecules. CoTPP, H_2TPP , and the gas-adsorbed one showed twofold symmetry instead of four-fold due to adsorption-induced deformations of saddle-shapes [45–47].

We performed STM single-molecule manipulation experiments using a voltage-sweep method to make assure if NH_3 or NO_2 were adsorbed to CoTPP not to H_2TPP . The STM tip was located at the center of a third molecule, and the sample voltage was increased while holding the feedback loop open so that the tip maintained a constant distance from the molecule. Figures 3(a) and 3(d) show current-voltage curves for manipulations of gas-adsorbed molecules in Figs. 2(b) and 2(d), with abrupt drops at 0.85 eV and 0.92 eV, respectively. The STM images obtained before the manipulations are shown in Figs. 3(b) and 3(e), and after the manipulations are shown in Figs. 3(c) and 3(f), respectively. STM images obtained in-between sequences of manipulations for NH_3 -adsorbed molecules are shown in Fig. S1 (see the Supplemental Material [48]). The images clearly show that the molecules obtained after the manipulations for both NH_3 and NO_2 are CoTPP. This implies that the third molecules are NH_3 -CoTPP and NO_2 -CoTPP, and that NH_3 and NO_2 molecules are de-coordinated from them by our manipulation procedures. The de-coordinated NH_3 and NO_2 may be desorbed, moved to a nearby CoTPP, or sometimes transferred to STM tip. In the third cases, we were able to move a NH_3 from the tip back to a CoTPP by the second manipulation procedures shown in Fig. S2 (see the Supplemental Material [48]), followed by the decoordination manipulations, with a voltage sweep from -0.5 to $+0.4 \text{ V}$. The central parts of NH_3 -CoTPP and NO_2 -CoTPP showed bright protrusion and rectangular shape, respectively [44].

To uncover the spin states and interactions in the system, we performed STS measurements at CoTPP, NH_3 -CoTPP, and NO_2 -CoTPP. Clear zero-bias peaks were obtained from

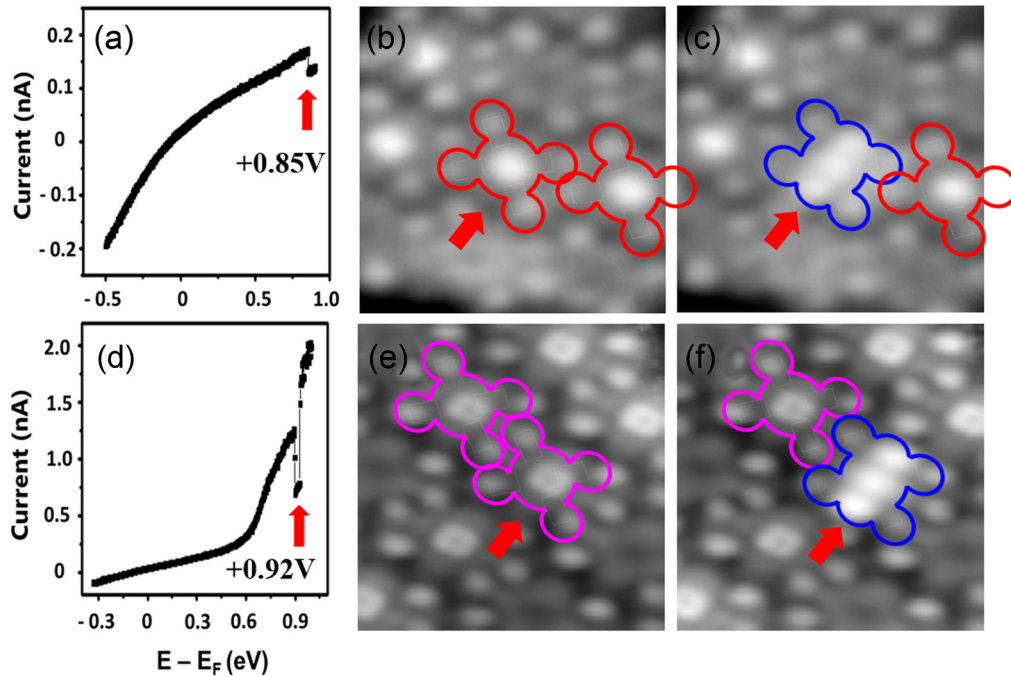


FIG. 3. Desorption of NH_3 and NO_2 from CoTPP. (a), (d) A current-voltage (I-V) curve obtained during STM manipulation procedure for (a) NH_3 and (d) NO_2 detachment. At the center of a gas-adsorbed porphyrin molecule, the sample bias was swept while holding the feedback loop open, resulting in an abrupt decrease in current at (a) +0.85 V and (d) +0.92 V. The STM images obtained (b) and (e) before and (c) and (f) after the STM manipulation of (a) and (d), respectively. The size of STM images: $4.5 \times 4.5 \text{ nm}^2$; tunneling current: $I_T = 0.1 \text{ nA}$; sample voltage: $V_S = -0.3 \text{ V}$.

both CoTPP and NH_3 -CoTPP, whereas no peak was resolved from NO_2 -CoTPP as shown in Fig. 4. The peaks are likely to originate from Kondo effect as discussed later [34,46,49–60]. The width of the peak from NH_3 -CoTPP is smaller than that from CoTPP, which implies that Kondo temperature is reduced in NH_3 -CoTPP. The Fano fitting is used to extract Kondo temperatures, 205 K from CoTPP and 135 K from NH_3 -CoTPP [61,62]. We performed STS measurement for 15 NH_3 -CoTPP complexes (see the Supplemental Material [48] for parts of them in Fig. S3) and averaged more than 50 times for each complex. The average Kondo temperature for NH_3 -CoTPP was $136 \pm 10 \text{ K}$. The effects of molecule-molecule interactions on Kondo resonance have been previously studied in similar systems [50,58]. In our case, the point STS was performed on molecules embedded at inner parts of large islands ($N > 20$), and they are surrounded by the same number of neighbors and environment. Although we were unable to observe significant variation of Kondo temperature for different atomic sites of Co and island sizes, it was still possible that CoTPP, NH_3 -CoTPP, and NO_2 -CoTPP included similar portions of molecule-molecule interactions.

To explain our experiments, we performed spin-polarized DFT calculations for CoTPP, NH_3 -CoTPP, and NO_2 -CoTPP/Au(111) using the Vienna *ab initio* simulation package (VASP) [63]. Plane waves with the kinetic energy cut-off of 400 eV, projector-augmented wave (PAW) potentials [64], and the Perdew-Burke-Ernzerhof (PBE) [65] exchange-correlation functional were used for our DFT simulations. For Au(111) slab model, we used the $p(6 \times 6)$ surface unit cell (36 surface Au atoms) and three atomic layers. The top layer of the Au substrate is fully relaxed with atomic forces less than

0.02 eV/\AA . $2 \times 2 \times 1$ Monkhorst-Pack k -point sampling is used. The work function of the Au(111) slab was calculated to be 5.29 eV, which is very close to experimental values of 5.1–5.5 eV [66]. The van der Waals interaction of gas-adsorbed CoTPP with Au(111) was corrected with DFT-D2 method [67].

Figures 5(a) and 5(c) show sideview structures of the DFT-optimized NH_3 and NO_2 -CoTPP/Au(111), respectively. It was found that NH_3 formed umbrellalike and NO_2 formed Y-shaped coordination to CoTPP, in agreement with previous theoretical and experimental reports [15,35,36,68,69]. The calculated binding energy between NH_3 and CoTPP is 0.64 eV and that between NO_2 and CoTPP is 1.86 eV. From molecular-orbital analysis, it was realized that the adsorption geometries stemmed from orbital hybridization between the Co- d_{z^2} and lone pair states of NH_3 - p_z and NO_2 - p_z . The orbital hybridization for NH_3 is relatively weak, because the Co- d_{z^2} is half occupied, whereas the NH_3 - p_z is fully occupied. In contrast, the orbital hybridization for NO_2 is relatively strong, because there is one electron transfer from CoTPP to NO_2 and thus Co- d_{z^2} becomes empty after coordination. An important finding from our calculations is that the distance between Co and Au(111) increases from 3.02 to 3.20 Å with NH_3 coordination and to 3.28 Å with NO_2 coordination. It is the manifestation of the trans effect that an existing bond (Co-Au) is weakened due to the introduction of an additional bond (Co-N) to the Co atom [1–5]. In our experiments, we observed that both NH_3 and NO_2 predominantly adsorbed to CoTPP; however, in some few occasions, we also observed that a lower pyrrole looked brighter than upper pyrroles in H_2 TPP after NO_2 exposure. There were many literatures that reported

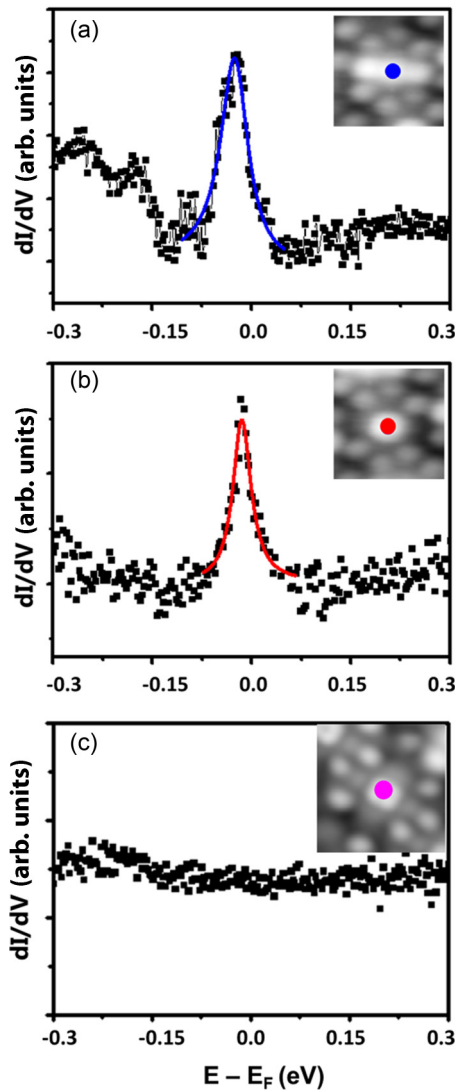


FIG. 4. Kondo resonance peaks. (a)–(c) Scanning tunneling spectroscopy spectra for (a) CoTPP, (b) NH_3 -CoTPP, and (c) NO_2 -CoTPP obtained at the center of three individual CoTPP, NH_3 -CoTPP, and NO_2 -CoTPP denoted in the insets. The initial tunneling conditions are $I_T = 0.1$ nA and Sample voltage: $V_S = -0.25$ V. The blue and red solid lines show a Fano fitting. The fitting parameters for the blue solid lines are $q = 14$, $\epsilon_K = -24$ meV, and $T_K = 205$ K. The fitting parameters for the red solid lines are $q = 55$, $\epsilon_K = -15$ meV, and $T_K = 135$ K. (Fitting formulas are in supporting information).

that the adsorption of NO_2 to the Langmuir-Blodgett films of H_2 TPP could be used for sensing applications for toxic NO_2 gas [70–72]. A DFT calculation predicted that NO_2 could adsorb to a lower pyrrole of H_2 TPP [72]. The reason why we could not observe large enough number of NO_2 adsorbed to H_2 TPP might be because of its relatively low binding energy (about 0.1 eV) compared with the case of CoTPP (1.86 eV).

In Figs. 5(b) and 5(d), electronic partial densities of states (PDOS) are plotted to denote molecular orbitals that carry unpaired electrons for NH_3 -CoTPP and NO_2 -CoTPP, respectively. Our DFT calculation results show that NH_3 -CoTPP is magnetic with the spin moment of $0.95 \mu_B$, whereas NO_2 -CoTPP is nonmagnetic with zero spin moment. Thus, the spin

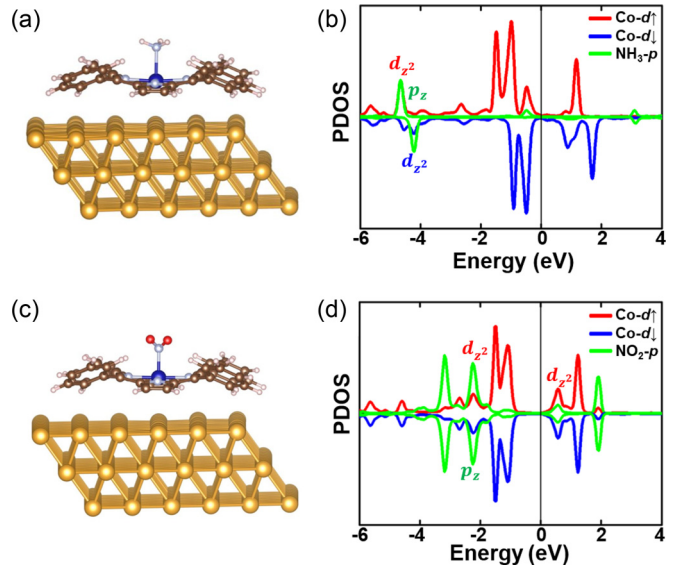


FIG. 5. Calculated geometric and electronic structures. (a), (c) DFT stabilized atomic model of vertical coordinated (a) NH_3 and (c) NO_2 molecules on Au-supported CoTPP molecule. (b), (d) Partial density of states (PDOS) for the coordinated molecule. The Fermi level is set to be zero. Red and blue lines indicate majority and minority spin of Co d -orbital, respectively. Green lines indicate spin (b) NH_3 and (d) NO_2 p -orbital.

moment of CoTPP remains nonvanishing during coordination reactions of NH_3 but becomes vanishing with coordination of NO_2 . The equal-spin-density surfaces are plotted to show the spatial distribution of spin in CoTPP and NH_3 -CoTPP in Figs. 6(a) and 6(c), respectively, and integrated spin densities along z axis are also plotted in Figs. 6(b) and 6(d). The spin is mostly distributed over the Co atom implying that its origin lies in its d_{z^2} orbitals. Only a part of the spin (less

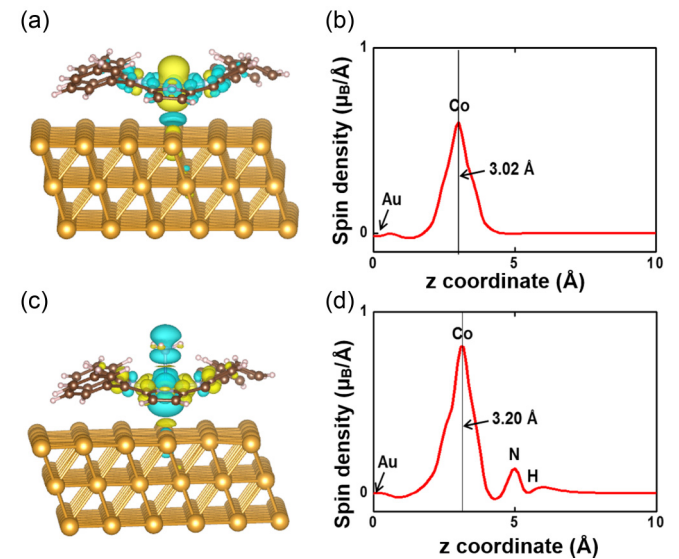


FIG. 6. Calculated spin distributions. (a), (c) Calculated spatial spin density plots for (a) CoTPP and (c) NH_3 -CoTPP molecule. (b), (d) Integrated spin density plot along the z axis for (b) CoTPP and (d) NH_3 -CoTPP molecule. The z coordinate zero means the top Au atom position.

than 10%) is located at NH_3 , as shown in Fig. 6(d) due to the spin-split lone-pair state. The coordination of NH_3 to the Co atom occurs with weak coupling and marginal charge donation. Based on the calculation results that both CoTPP and NH_3 -CoTPP are magnetic, we can infer that the zero-bias peaks observed in CoTPP and NH_3 -CoTPP/Au(111) are the signatures of Kondo effect, the interaction between a localized spin in a molecule and delocalized spins in Au(111).

The reason why the Kondo temperature of NH_3 -CoTPP/Au(111) is reduced from that of CoTPP/Au(111) can be explained with the increased distance between Co and Au. In Kondo perturbation theory, the Kondo temperature (T_K) is the functions of width of conduction band (D), electron density of state of conduction electrons (ρ), and spin-spin exchange coupling constant (J), namely, $k_B T_K = D \cdot \exp(-\rho \cdot J)$ [73,74]. Thus, as the distance between Co and Au increases, the coupling constant J will decrease, resulting in the reduced Kondo temperature. Numerical renormalization-group (NRG) calculations for a two-orbital Anderson model consisting of an interacting d -orbital, finite Coulomb interaction, and a noninteracting molecular orbital coupled to a metallic surface have been reported by Luis et al. for Co-porphyrin on Cu(111) [75]. Although it was performed with different substrate, the results of model NRG calculations using DFT-determined inputs such as d -orbitals energies and the distance between Co and substrate can be considered in our systems. Their calculation results indeed showed that the Kondo temperature was exponentially dependent on the distance between Co and metal substrate and d -orbital energies. When the d -orbital was in the range between -0.6 and -0.8 eV, the Kondo temperatures for the Co which were 3.02 and 3.20 Å away from substrate stayed in the range between 200 and 100 K, and was reduced roughly by 50% , showing reasonable agreement with our experimental observations. Therefore, the reduced Kondo temperature from our experiments can be explained with the increased distance between unpaired spin and Au(111). It would be helpful if one directly measures the distance between Co and Au for each cases. From the fitting of x-ray standing wave (XSW) absorption profiles performed on self-assembly-film, their distance can be experimentally extracted and compared with DFT calculation results [22].

III. CONCLUSION

In summary, we studied spin trans effect of CoTPP/Au(111) with coordination of NH_3 and NO_2

using STM and STS measurement. We observed clear zero-bias peaks from both CoTPP and NH_3 -CoTPP/Au(111), which can be ascribed as Kondo resonances based on our DFT calculation results, whereas no zero-bias peak from NO_2 -CoTPP. The reduced Kondo temperature in NH_3 -CoTPP/Au(111) and switching-off of Kondo resonance in NO_2 -CoTPP are explained with the spatial redistribution of unpaired spins in d_{z^2} orbitals of Co-porphyrin by NH_3 and NO_2 coordination, respectively. Thus, our study shows the spin interactions of CoTPP and Au(111) can be marginally reduced with NH_3 coordination, as well as abruptly switched off with NO_2 coordination at the single molecule level. Because there are huge numbers of sets for magnetic metallomolecules and gaseous small molecules, the methods we show in this report can be performed with different sets to explore further controllability.

IV. METHODS

Experiments were performed using our home-built STM system operating at 80 or 10 K with a base pressure of 1×10^{-10} Torr. The Au(111) surface was prepared from a commercially available thin film (200 nm thick, PHASIS, Switzerland) of Au on mica that was exposed to several cycles of Ne-ion sputtering and annealing at 800 K. A mixture of commercially available CoTPP (Porphyrin Systems, Germany) and H_2 TPP (Sigma Aldrich, USA) was outgassed in vacuum for several hours and then deposited on the Au(111) at submonolayer coverage by thermal evaporation using an alumina-coated evaporator. NH_3 and NO_2 gas were introduced using a stainless steel tube (3 -mm diameter) through a precision leak valve. STS spectra were obtained by a lock-in technique with a modulation voltage of $5 \text{ mV}_{\text{rms}}$ and at a frequency of 1.5 kHz.

ACKNOWLEDGMENTS

The authors gratefully acknowledge financial support from the National Research Foundation of Korea (Grants No. 2017R1A2A2A05069833, No. 2018R1A6A3A11043228, and No. 2018R1A4A1024157), and Korea University Grants. Work at KAIST was supported by the NRF (Grant No. 2018R1A2A2A14079326), SRC (Grant No. 2016R1A5A1008184), and Global Frontier R&D (Grant No. 2011-0031566) programs of Korea.

-
- [1] R. H. Crabtree, *The Organometallic Chemistry of the Transition Metals* (Wiley, New Jersey, 2005).
 - [2] I. I. Chernyaev, I. Ann. Inst. Platine (USSR) **4**, 243 (1926).
 - [3] J. V. Quagliano and L. E. O. Schubert, *Chem. Rev.* **50**, 201 (1952).
 - [4] F. R. Hartley, *Chem. Soc. Rev.* **2**, 163 (1973).
 - [5] B. J. Coe and S. J. Glenwright, *Coord. Chem. Rev.* **203**, 5 (2000).
 - [6] K. Flechtner, A. Kretschmann, H. P. Steinruck, and J. M. Gottfried, *J. Am. Chem. Soc.* **129**, 12110 (2007).
 - [7] N. L. Tran and A. C. Kummel, *J. Chem. Phys.* **127**, 214701 (2007).
 - [8] M. Gottfried and H. Marbach, *Z. Physik. Chem.* **223**, 53 (2009).
 - [9] G. S. S. Saini, S. Sukhwinder, K. Sarvpreet, K. Ranjan, S. Vasant, and S. K. Tripathi, *J. Phys. Condens. Matter* **21**, 225006 (2009).

- [10] K. Seufert, W. Auwaerter, and J. V. Barth, *J. Am. Chem. Soc.* **132**, 18141 (2010).
- [11] S. A. Suarez, M. H. Fonticelli, A. A. Rubert, E. de la Llave, D. Scherlis, R. C. Salvarezza, M. A. Marti, and F. Doctorovich, *Inorg. Chem.* **49**, 6955 (2010).
- [12] W. Hieringer, K. Flechtner, A. Kretschmann, K. Seufert, W. Auwaerter, J. V. Barth, A. Gorling, H. P. Steinruck, and J. M. Gottfried, *J. Am. Chem. Soc.* **133**, 6206 (2011).
- [13] C. Isvoranu, J. Knudsen, E. Ataman, K. Schulte, B. Wang, M.-L. Bocquet, J. N. Andersen, and J. Schnadt, *J. Chem. Phys.* **134**, 114711 (2011).
- [14] C. Isvoranu, B. Wang, E. Ataman, J. Knudsen, K. Schulte, J. N. Andersen, M. L. Bocquet, and J. Schnadt, *J. Phys. Chem. C* **115**, 24718 (2011).
- [15] C. Isvoranu, B. Wang, E. Ataman, K. Schulte, J. Knudsen, J. N. Andersen, M.-L. Bocquet, and J. Schnadt, *J. Chem. Phys.* **134**, 114710 (2011).
- [16] K. Seufert, M.-L. Bocquet, W. Auwärter, A. Weber-Bargioni, J. Reichert, N. Lorente, and J. V. Barth, *Nat. Chem.* **3**, 114 (2011).
- [17] B. A. Friesen, A. Bhattarai, U. Mazur, and K. W. Hipps, *J. Am. Chem. Soc.* **134**, 14897 (2012).
- [18] N. Ballav, C. Wackerlin, D. Siewert, P. M. Oppeneer, and T. A. Jung, *J. Phys. Chem. Lett.* **4**, 2303 (2013).
- [19] B. E. Murphy, S. A. Krasnikov, N. N. Sergeeva, A. A. Cafolla, A. B. Preobrajenski, A. N. Chaika, O. Luebben, and I. V. Shvets, *ACS Nano* **8**, 5190 (2014).
- [20] J. H. Park, P. Choudhury, and A. C. Kummel, *J. Phys. Chem. C* **118**, 10076 (2014).
- [21] J. L. Zhang, Z. Wang, J. Q. Zhong, K. D. Yuan, Q. Shen, L. L. Xu, T. C. Niu, C. D. Gu, C. A. Wright, A. Tadich, D. Qi, H. X. Li, K. Wu, G. Q. Xu, Z. Li, and W. Chen, *Nano Lett.* **15**, 3181 (2015).
- [22] P. S. Deimel, R. M. Bababrik, B. Wang, P. J. Blowey, L. A. Rochford, P. K. Thakur, T.-L. Lee, M.-L. Bocquet, J. V. Barth, D. P. Woodruff, D. A. Duncan, and F. Allegretti, *Chem. Sci.* **7**, 5647 (2016).
- [23] J. M. Kamm, C. P. Iverson, W. Y. Lau, and M. D. Hopkins, *Langmuir* **32**, 487 (2016).
- [24] T. Knaak, T. G. Gopakumar, B. Schwager, F. Tuczek, R. Robles, N. Lorente, and R. Berndt, *J. Am. Chem. Soc.* **138**, 7544 (2016).
- [25] G. Nandi, B. Chilukuri, K. W. Hipps, and U. Mazur, *PCCP* **18**, 20819 (2016).
- [26] D. Nguyen, G. Kang, N. Chiang, X. Chen, T. Seideman, M. C. Hersam, G. C. Schatz, and R. P. Van Duyne, *J. Am. Chem. Soc.* **140**, 5948 (2018).
- [27] C. Isvoranu, B. Wang, K. Schulte, E. Ataman, J. Knudsen, J. N. Andersen, M. L. Bocquet, and J. Schnadt, *J. Phys. Condens. Matter* **22**, 472002 (2010).
- [28] C. Wackerlin, D. Chylarecka, A. Kleibert, K. Muller, C. Iacovita, F. Nolting, T. A. Jung, and N. Ballav, *Nat. Commun.* **1**, 61 (2010).
- [29] J. Miguel, C. F. Hermanns, M. Bernien, A. Krüger, and W. Kuch, *J. Phys. Chem. Lett.* **2**, 1455 (2011).
- [30] C. F. Hermanns, M. Bernien, A. Krüger, J. Miguel, and W. Kuch, *J. Phys. Condens. Matter* **24**, 394008 (2012).
- [31] A. Stróżecka, M. Soriano, J. I. Pascual, and J. J. Palacios, *Phys. Rev. Lett.* **109**, 147202 (2012).
- [32] C. Wackerlin, K. Tarafder, D. Siewert, J. Girovsky, T. Hählen, C. Iacovita, A. Kleibert, F. Nolting, T. A. Jung, P. M. Oppeneer, and N. Ballav, *Chem. Sci.* **3**, 3154 (2012).
- [33] C. F. Hermanns, M. Bernien, A. Krüger, W. Walter, Y.-M. Chang, E. Weschke, and W. Kuch, *Phys. Rev. B* **88**, 104420 (2013).
- [34] H. Kim, Y. H. Chang, S. H. Lee, Y. H. Kim, and S. J. Kahng, *ACS Nano* **7**, 9312 (2013).
- [35] C. Wackerlin, J. Nowakowski, S.-X. Liu, M. Jaggi, D. Siewert, J. Girovsky, A. Shchyrba, T. Hählen, A. Kleibert, P. M. Oppeneer, F. Nolting, S. Decurtins, T. A. Jung, and N. Ballav, *Adv. Mater.* **25**, 2404 (2013).
- [36] C. Wackerlin, K. Tarafder, J. Girovsky, J. Nowakowski, T. Hählen, A. Shchyrba, D. Siewert, A. Kleibert, F. Nolting, P. M. Oppeneer, T. A. Jung, and N. Ballav, *Angew. Chem. Int. Ed.* **52**, 4568 (2013).
- [37] H. Kim, Y. H. Chang, S. H. Lee, S. Lim, S. K. Noh, Y. H. Kim, and S. J. Kahng, *Chem. Sci.* **5**, 2224 (2014).
- [38] N. Tsukahara, E. Minamitani, Y. Kim, M. Kawai, and N. Takagi, *J. Chem. Phys.* **141**, 054702 (2014).
- [39] H. Kim, Y. H. Chang, W.-J. Jang, E.-S. Lee, Y.-H. Kim, and S.-J. Kahng, *ACS Nano* **9**, 7722 (2015).
- [40] Y. H. Chang, H. Kim, S. J. Kahng, and Y. H. Kim, *Dalton Trans.* **45**, 16673 (2016).
- [41] N. Hatter, B. W. Heinrich, D. Rolf, and K. J. Franke, *Nat. Commun.* **8**, 2016 (2017).
- [42] W. Kuch and M. Bernien, *J. Phys. Condens. Matter* **29**, 023001 (2017).
- [43] Y. Wang, X. Li, X. Zheng, and J. Yang, *J. Chem. Phys.* **147**, 134701 (2017).
- [44] M. H. Chang, N. Y. Kim, Y. H. Chang, Y. Lee, U. S. Jeon, H. Kim, Y.-H. Kim, and S.-J. Kahng, *Nanoscale* **11**, 8510 (2019).
- [45] A. Weber-Bargioni, W. Auwärter, F. Klappenberger, J. Reichert, S. Lefrançois, T. Strunskus, C. Wöll, A. Schiffrin, Y. Pennec, and J. V. Barth, *Chem. Phys. Chem.* **9**, 89 (2008).
- [46] H. Kim, W.-j. Son, W. J. Jang, J. K. Yoon, S. Han, and S.-J. Kahng, *Phys. Rev. B* **80**, 245402 (2009).
- [47] W. Auwärter, K. Seufert, F. Klappenberger, J. Reichert, A. Weber-Bargioni, A. Verdini, D. Cvetko, M. Dell'Angela, L. Floreano, A. Cossaro, G. Bavdek, A. Morgante, A. P. Seitsonen, and J. V. Barth, *Phys. Rev. B* **81**, 245403 (2010).
- [48] See Supplemental Material at <http://link.aps.org/supplemental/10.1103/PhysRevB.100.245406> for additional results and discussions.
- [49] A. Zhao, Q. Li, L. Chen, H. Xiang, W. Wang, S. Pan, B. Wang, X. Xiao, J. Yang, J. G. Hou, and Q. Zhu, *Science* **309**, 1542 (2005).
- [50] V. Iancu, A. Deshpande, and S.-W. Hla, *Phys. Rev. Lett.* **97**, 266603 (2006).
- [51] V. Iancu, A. Deshpande, and S.-W. Hla, *Nano Lett.* **6**, 820 (2006).
- [52] Y.-S. Fu, S.-H. Ji, X. Chen, X.-C. Ma, R. Wu, C.-C. Wang, W.-H. Duan, X.-H. Qiu, B. Sun, P. Zhang, J.-F. Jia, and Q.-K. Xue, *Phys. Rev. Lett.* **99**, 256601 (2007).
- [53] L. Gao, W. Ji, Y. B. Hu, Z. H. Cheng, Z. T. Deng, Q. Liu, N. Jiang, X. Lin, W. Guo, S. X. Du, W. A. Hofer, X. C. Xie, and H. J. Gao, *Phys. Rev. Lett.* **99**, 106402 (2007).
- [54] A. Zhao, Z. Hu, B. Wang, X. Xiao, J. Yang, and J. G. Hou, *J. Chem. Phys.* **128**, 234705 (2008).
- [55] Q. Li, S. Yamazaki, T. Eguchi, H. Kim, S. J. Kahng, J. F. Jia, Q. K. Xue, and Y. Hasegawa, *Phys. Rev. B* **80**, 115431 (2009).

- [56] T. Choi, S. Bedwani, A. Rochefort, C.-Y. Chen, A. J. Epstein, and J. A. Gupta, *Nano Lett.* **10**, 4175 (2010).
- [57] T. Komeda, H. Isshiki, J. Liu, Y.-F. Zhang, N. Lorente, K. Katoh, B. K. Breedlove, and M. Yamashita, *Nat. Commun.* **2**, 217 (2011).
- [58] N. Tsukahara, S. Shiraki, S. Itou, N. Ohta, N. Takagi, and M. Kawai, *Phys. Rev. Lett.* **106**, 187201 (2011).
- [59] J.-P. Gauyacq, N. Lorente, and F. D. Novaes, *Prog. Surf. Sci.* **87**, 63 (2012).
- [60] L. Liu, K. Yang, Y. Jiang, B. Song, W. Xiao, L. Li, H. Zhou, Y. Wang, S. Du, M. Ouyang, W. A. Hofer, A. H. Castro Neto, and H.-J. Gao, *Sci. Rep.* **3**, 1210 (2013).
- [61] U. Fano, *Phys. Rev.* **124**, 1866 (1961).
- [62] K. Nagaoka, T. Jamneala, M. Grobis, and M. F. Crommie, *Phys. Rev. Lett.* **88**, 077205 (2002).
- [63] G. Kresse and J. Furthmüller, *Comput. Mater. Sci.* **6**, 15 (1996).
- [64] P. E. Blöchl, *Phys. Rev. B* **50**, 17953 (1994).
- [65] J. P. Perdew, K. Burke, and M. Ernzerhof, *Phys. Rev. Lett.* **77**, 3865 (1996).
- [66] C.-T. Tseng, Y.-H. Cheng, M.-C. M. Lee, C.-C. Han, C.-H. Cheng, and Y.-T. Tao, *Appl. Phys. Lett.* **91**, 233510 (2007).
- [67] S. Grimme, *J. Comput. Chem.* **27**, 1787 (2006).
- [68] W. Zhao, D. Zou, Z. Sun, Y. Yu, and C. Yang, *Phys. Lett. A* **382**, 2666 (2018).
- [69] D. Zou, W. Zhao, B. Cui, D. Li, and D. Liu, *Phys. Chem. Chem. Phys.* **20**, 2048 (2018).
- [70] T. H. Richardson, C. M. Dooling, L.T. Jones, and R. A. Brook, *Adv. Colloid Interface Sci.* **116**, 81 (2005).
- [71] R. Paolesse, S. Nardis, D. Monti, M. Stefanelli, and C. Di Natale, *Chem. Rev.* **117**, 2517 (2017).
- [72] M. Rivera, J. M. Rivera, O. Amelines-Sarria, and Y. A. Wang, *Adv. Mater. Phys. Chem.* **8**, 441 (2018).
- [73] A. C. Hewson, *The Kondo Problem to Heavy Fermions* (Cambridge University Press, Cambridge, UK, 1993).
- [74] N. Knorr, M. A. Schneider, L. Diekhöner, P. Wahl, and K. Kern, *Phys. Rev. Lett.* **88**, 096804 (2002).
- [75] L. G. G. V. Dias da Silva, M. L. Tiago, S. E. Ulloa, F. A. Reboredo, and E. Dagotto, *Phys. Rev. B* **80**, 155443 (2009).